Experimental Analysis of Dragonfly-Inspired Airfoils at Re = 4000

Group 24: Marko Danial, Andy Glover, Josh Liao, Alex Suvorov

Dept. of Aerospace and Mechanical Engineering, University of Southern California.

Motivation

- **Objective:** Evaluate the lift of airfoils that mimic the cross-section of dragonfly wings.
- Assess bio-inspired designs for practical aerodynamic advantages.
- Identify optimal corrugation pattern that improves aerodynamic efficiency for applications in micro air vehicles (MAVs), unmanned aerial vehicles (UAVs)

Figure 1: *"Dragonflies see the world in slow motion" via BBC Earth show Super Senses.*

- Study will determine if an alternative cross section geometry alone can achieve increased lift compared to a conventional NACA airfoil, even without using the additional spanwise effects present in actual dragonfly wings.

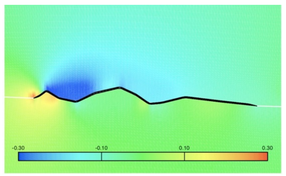

Figure 2: *Pressure distribution of corrugated airfoil of 2° α, Re = 4000, from numerical simulation by Tang et al [1].*

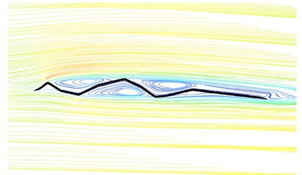

Figure 3: *Streamlines around corrugated airfoil of 2° α, Re = 4000 from numerical simulation by Tang et al [1].*

- The CFD study by Tang et al. [1], which inspired this analysis, suggests that corrugation valleys generate lower pressure regions compared to conventional NACA airfoils in laminar ($Re = 4000$) flow.

Theory & Expectations

- **Hypothesis:** Dragonfly-inspired designs will outperform (greater C_L at various angles of attack, α) smooth airfoils like the NACA 2408/2410 in low Reynolds number conditions.

$$\boldsymbol{Re = 4000 \implies Sizing\ Equations}$$

Lift Coefficient

$$C_L = \frac{F_L}{\frac{1}{2}\rho {U_0}^2 S}$$

F_L: Lift Force
ρ: Density of water
U_0: Flow Speed (m/s)
S: Wing Area

Beam Deflection

$$\delta = \frac{F_L L^3}{3EI}$$

F_L: Lift Force
L: Beam Length
E: Modulus of Elasticity
I: Moment of Inertia

- Using the equations above, the expected maximum lift force and beam deflection were calculated:

$\boldsymbol{F_L \approx 20\ mN}$ $\boldsymbol{\delta \approx 9\ cm}$

- Two notable design constraints were water channel flow speed (~$4\ cm/s$) and height limit for frame (part length and structural stability).
- Sufficient deflection achieved for ~ $1\ mV$ data resolution for measurements by a strain gauge with a Wheatstone bridge.

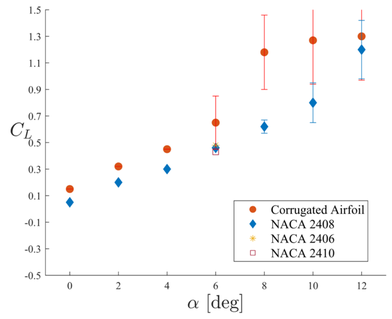

Figure 6: Replicated numerical data from Tang et al [1] showing an improvement in C_L vs. α for the dragonfly inspired wing.

Results

- Strain gauge experimental data shown below in Figure 7.

Initial Observations & Comments

- Increase in the mean C_L values for corrugated airfoils as predicted by Tang et al [1] and Deubel et al [2].
- Higher uncertainties lead by fluctuations in water flow.
- As seen in the next section, flow is not as laminar as would be expected for $Re = 4000$ flow.
- Low pass filter using MATLAB butter function was implemented to eliminate noise in signal.
- Highest increase in C_L mean values exists in the region < 6°, indicating the corrugation has a larger impact as a form of camber instead of reducing boundary layer separation, also expected by Tang et al [1].
- Universal C_L decrease for extreme airfoil.

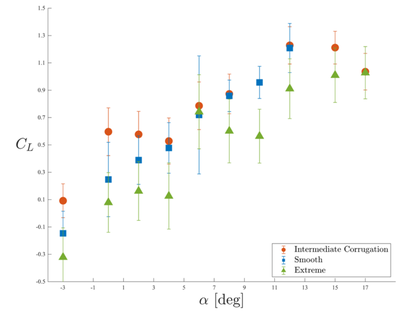

Figure 7: *C_L vs. α from the experiment using the strain gauge deflection measurements.*

- Blue dye inserted in the freestream flow and captured in the profile view:
- Regions of recirculation in the two upper valleys shown in Fig. 9, matches expectation.
- Tip (left) of corrugation "trips" the boundary layer and the low-pressure circulation settles in the aft-ward valley [2].

Figure 8: *Expected recirculation phenomenon for a simplified dragonfly wing [3].*

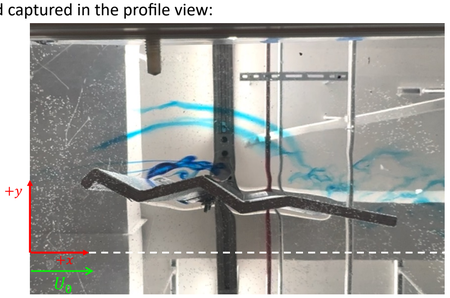

Figure 9: *Flow visualization and physical beam deflection measurement method for the intermediate corrugation at α = 3° .*

Design

- Three airfoils: **Smooth** (NACA 2410 control), **Intermediate Corrugation** (matches dragonfly wing coordinates from Tang et al [1]), **Extreme Corrugation** (two intermediate corrugation sections compressed into the length of one).

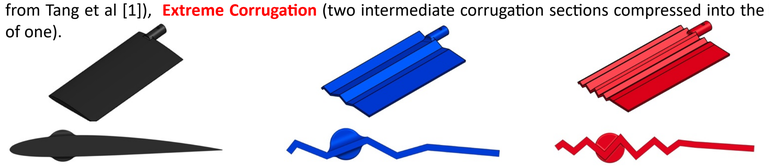

- Airfoils: $20\ cm$ chord, $200\ mm$ span, and $3\ mm$ thickness, 3D printed in PETG for durability and precision.
- Cantilever Beam: Aluminum 6061, measuring $551\ mm$ in length, $15\ mm$ in width, and $1.02\ mm$ in thickness.
- Frame: 1.5" aluminum t-slots, $129\ cm$ tall, positioning the airfoil above the water channel surface.
- Setup: Airfoil mounted to a cantilever beam for deflection-based force measurements.

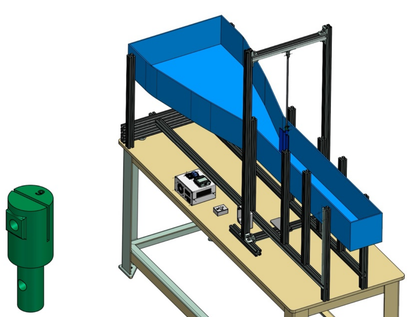

Angle of Attack (*AoA* or α) Connectors: Custom 3D-printed ABS pieces that enable testing from $-3°$ to $18°$.

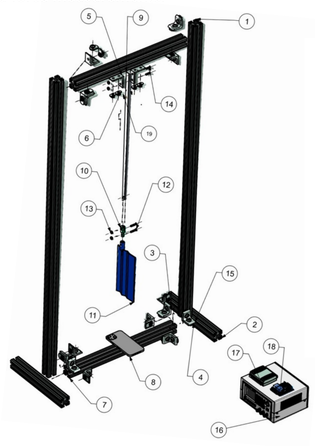

Experiment

- Calibration:
  - Incrementally applied weights verified the force-voltage relationship using a Wheatstone Bridge circuit.
- Flow Visualization:
  - Dye introduced into the water channel highlighted flow separation and vortex formation in the valleys of the corrugations.
- Setup:
  - Experiments conducted in USC's Small Water Channel in the Rapp Engineering Building (RRB).
  - Strain gauges (Omega SGD-6/120-LY13).
- Data Processing:
  - Voltages measured by strain gauges and LabView VI are calculated into a force using calibration slope, then lift coefficient C_L and deflection δ can be calculated using that force.
- Setbacks:
  - The motor for the water channel was not crimped properly, causing frequency to fluctuate immensely in some cases and altering the consistent Reynolds number of 4000 needed in the water channel.

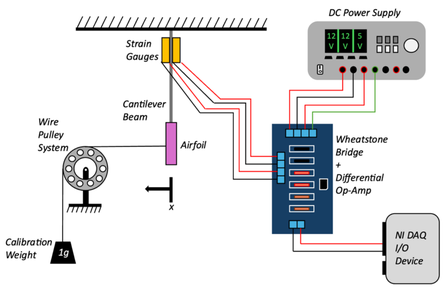

Figure 4: *Diagram of electronics used for the strain gauge measurements (shown above with the additional equipment used in the calibration)*

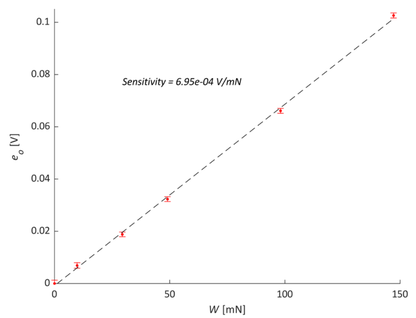

Figure 5: *Results of strain gauge calibration testing as shown in Fig. 4 – airfoil loading related to the generated strain gauge voltage.*

Conclusion & Future Work

Key Findings:

- The largest increase in C_L occurs between 0° to 6 (Fig. 7), as suggested by Tang et al [1].
- ***Noteworthy:*** Lift is not linear before stall angle for the intermediate corrugation.
- Uncertainties in flow speed from the water channel and beam oscillation cause overlap in smooth vs. intermediate corrugation despite visibly different mean values.
- Vorticity in the two valleys of the upper surface matches predictions from Tang et al.'s numerical CFD (Fig. 9).
- Decrease in extreme performance likely due to stalling in downstream valleys.

Future Work:

- Increase the scale of the wing, flow speed (maintaining Re = 4000) for more detectable drag forces for (L/D).
- Change water channel impeller for more stable velocity readings.
- Conduct particle image velocimetry (PIV) to capture more precise flow patterns.
- Explore real-world applications in UAVs and underwater drones.

Acknowledgements & References

Special thanks to Dr. Emma Singer and Dr. Mitul Luhar for their guidance, and to Usiel Ulloa for his assistance with 3D printing. We also thank the entire USC AME 441 Lab staff for their support.

[1] H. Tang, Y. Lei, X. Li, and Y. Fu, 'Numerical Investigation of the Aerodynamic Characteristics and Attitude Stability of a Bio-Inspired Corrugated Airfoil for MAV or UAV Applications', Energies, vol. 12, p. 4021, 10 2019.
[2] T. Deubel, S. Wanke, C. Weber, and F. Wedekind, 'Modelling and Manufacturing of a Dragonfly Wing as Basis for Bionic Research', *Strojarstvo*, vol. 49, 01 2008.
[3] Hien, K., Kesel, A. B., Wedekind, F., "Umströmungs-Visualisierung und aerodynamische Effekte der Profilierung des Libellenflügels", BIONA Report 10, Nachtigall, W., Wisser, A., Saarbrücken, 1996.